

Deep Learning Ensemble Model for Hyperspectral Image Classification

¹Parul Bhanarkar, ²Dr. Salim Y. Amdani

^{1,2} Babasaheb Naik College of Engineering, Pusad, Maharashtra, India

ABSTRACT

Article Info

Volume 9, Issue 2

Page Number : 12-18

Publication Issue :

March-April-2022

Article History

Accepted : 02 March 2022

Published: 08 March 2022

Hyperspectral image catch exceptionally increasing data dimensionality about filtered objects and, henceforth, can be utilized to uncover different attributes of the materials present in the broke down scene. In any case, such picture information are hard to move because of their huge volume, and creating new ground-truth datasets that could be used to prepare regulated students is expensive, tedious, very userdependent, and regularly infeasible practically speaking. The examination endeavors have been zeroing in on creating calculations for hyperspectral information order and unmixing, which are two primary assignments in the investigation chain of such symbolism. Albeit in the two of them, the profound learning strategies have blossomed as a very viable apparatus, planning the profound models that sum up above and beyond the inconspicuous information is a not kidding viable test in arising applications. In this paper, we present the profound outfits profiting from various structural advances of convolution base models also propose another methodology towards totaling the results of base students utilizing an administered fuser.

Keywords : Ensemble , Classifier, hyperspectral , images, convolution, neural network.

I. INTRODUCTION

Hyperspectral images with many phantom channels play an increasingly more significant job in checking, biomedical also criminological [1]. In this manner, numerous well known strategies have been produced for the investigation of the hyperspectral picture. Among these techniques, profound strategies, which can separate conceptual and significant level elements, will quite often be an intriguing issue [2, 3]. In any case, the set number of preparing tests typically makes the learned model to be poor. Besides, various articles in

hyperspectral picture normally show comparative unearthly highlights which make it hard to extricate discriminative elements. This spurs investigating more compelling profound models for hyperspectral picture portrayal and grouping. Profound conviction organization (DBN) [4], which can utilize the unlabeled tests for pre-preparing and afterward the accessible labeled tests for calibrating on the pre-prepared model, is introduced into this work for hyperspectral picture grouping. Despite the fact that DBN can exploit unlabelled information, the mind boggling and comparative ghostly data between

various classes in hyperspectral picture actually make the learned DBN sub-par. To take care of the issue and further work on the representational capacity of the profound model, profound troupe technique is typically utilized. The profound troupe expects to get numerous decisions by isolating the preparation tests into various subsets, every one of which prepares a relating model. In any case, there actually exists numerous overt repetitiveness between the learned models and the entire presentation might even diminish due to the less of preparing tests for each model. In this work, a clever differentiated profound gathering in light of DBN is created for hyperspectral picture arrangement. We mean to differentiate the portrayal of items from different models. Earlier works have effectively proposed numerous ensemble variety techniques in numerous PC vision errands, such as regular picture division [5, 6, 7], machine interpretation [8]. In any case, the greater part of the earlier works center around differentiating different portrayal by adding earlier data as regularization. Like work [5], this work intends to energize each model to address just piece of the entire examples in the hyperspectral picture. Since each model just requirements to display less item classes, the authentic capacity of each model for these predefined classes is moved along. Accordingly, the entirety portrayal of the profound group is moved along. At long last, a exceptional data combination technique is proposed to acquire the last deduction.

II. LITERATURE SURVEY

In the past twenty years, hyperspectral images (HSIs) which acquired via different platforms have been gradually applied to different targets such as anomaly detection, land use land cover mapping and classification (Filippi et al. 2009; Jones et al. 2010). Compared with the multispectral remote sensing images, hyperspectral images have the characteristics of recording hundreds of contiguous narrow spectral bands which cover a large spectral wavelength range

from the visible to the infrared spectrum. It has double effects for the processing and applying of the HSIs. On the one hand, abundant spectral features contained within each pixel makes it possible to detect the tiny materials and subtle traits which are impossible to be observed by multispectral images acquired by Landsat TM/ ETM sensors and ASTER sensor. On the other hand, the issues of processing the high-dimension data which usually have several hundred bands brought many tough questions, for instance, the dimension reduction, feature extraction and classification (Harsanyi and Chang 1994; Lavanya and Sanjeevi 2012). Retrieval of the land use land cover (LULC) information from the HSIs using classification methods becomes one of the most important research hot areas in the field of remote sensing application (Chirici et al. 2011; Henriques et al. 2010; Huang et al. 2014; Myint et al. 2011; Pu and Landry Classification processing usually employs the features of materials, due to the fact that different materials have different reflections at a certain spectral band to identify the land use land cover type. Before extracting land use land cover information from HSIs, two issues, i.e., dimension reduction (Harsanyi and Chang 1994) and classification algorithm (Erener 2013), should be determined.

To overcome the high-dimensional problem, many dimension reduction methods have been proposed such as orthogonal subspace projection approach (Harsanyi and Chang 1994), principal component analysis (PCA) (Wei et al. 2015), linear discriminate analysis (LDA) and local linear embedding (LLE). PCA is one of the classical dimensional reduction approaches, and it tries to maximize the variance of the correlation matrix of the variables in an unsupervised way. Many classification methods have been proposed in the past thirty years trying to improve the classification among different materials such as handwriting recognition, texture classification, medical image recognition, video image classification and traffic management. There are some classical classifiers such as linear classifier, maximum likelihood

classifier and decision tree classifier (Chakraborty et al. 2016; Pu and Landry 2012), support vector machine (SVM) classifier (Gu and Sheng 2016; Gu et al. 2015; Filippi et al. 2009; Habib et al. 2009; Turker and Koc-San 2015; Volpi et al. 2013), artificial neural network classifier (Han et al. 2012; Pacifici et al. 2009). It has been found that weak classifiers such as linear classifier and maximum likelihood classifier lead to poor classification results compared with the results derived from those strong classifiers, for instance, the SVM and decision tree classifier.

Efforts to improve the classification accuracy always are made along two different ways. The first one is to modify or tune those strong classifiers such as SVM and random forest classifier. Based on the margin maximization principle, SVM approaches have been proved particularly promising for the mapping of land use land cover from remotely sensed images (Huang and Zhang 2010, 2013; Huang et al. 2014). The principle provided an opportunity for us to modify or generalize it further to improve the performance of classification under different conditions (Ghoggali and Melgani 2008; Gu and Sheng 2016; Gu et al. 2015; Filippi et al. 2009; Habib et al. 2009; Turker and Koc-San 2015; Volpi et al. 2013). Meanwhile, ensemble classification is another way which tries to assemble the classification results derived from multiple weak classifiers. Weak classifiers, such as linear classifier, extreme learning machine, artificial neural network, usually generate poor classification results. However, it had been verified that higher classification accuracy could be attained through the ensemble classification. Ensemble Classification Ensemble classification is a relatively novel strategy proposed in the past twenty years (Zhang et al. 2016; Chi et al. 2009; Han et al. 2012; Henriques et al. 2010; Huang and Zhang 2013) which integrate multiple weak classifiers to get an improved classification results compared with the results of a single classifier. Three levels of ensemble method could be concluded: data-level combination, feature-level combination and classifier-level combination. Data-level combination means to resample different

training data sets for base classifiers, and then the results are combined to get the final results. Feature-level combination refers to the randomly selection of different feature subsets and the combination of classification results. Classifierlevel combination suggests that different or same types of classifiers are trained using same data sets and combined to obtain classifier results (Uslu et al. 2016). Flexibility and higher accuracy of ensemble classification attracted many researchers to explore its application in many fields. Many researches about ensemble learning and classification focus on the strategy of training different weak classifiers such as artificial neural network classifier and linear classifier

III. DATASET

ROSIS Pavia University Hyperspectral Image: Reflective optics spectrographic image system (ROSIS) Pavia University hyperspectral image was acquired with ROSIS optical sensor which provides 115 bands with a spectral range coverage ranging from 0.43 to 1 μ . The spatial resolution is 1.3 m. The each image has pixels with 103 spectral channels and 9 classes were considered.










Class	Description	GT Color	Number of Samples
1	Asphalt		6631
2	Meadows		18,649
3	Gravel		2099
4	Trees		3064
5	Painted metal sheets		1345
6	Bare Soil		5029
7	Bitumen		1330
8	Self-Blocking Bricks		3682
9	Shadows		947
Total			42,776

Table-1 : Class and sample description ROSIS Pavia University Hyperspectral Image

Kennedy Space Center (KSC) Hyperspectral Image: KSC hyperspectral image shown in Fig. 1(e) was acquired with airborne visible/infrared imaging spectrometer (AVIRIS) sensor over the Kennedy Space Center (KSC), Florida, USA, on March 23, 1996. This image has 224 bands from 400 to 2500 nm and the

spatial resolution is 18 m. After removing water absorption and low signal-to-noise (SNR) bands, it has pixels with 176 bands. Thirteen classes are used for this site.

Class	Description	GT Color	Number of Samples
1	Healthy grass		39,196
2	Stressed grass		130,008
3	Artificial turf		2736
4	Evergreen trees		54,322
5	Deciduous trees		20,172
6	Bare earth		18,064
7	Water		1064
8	Residential buildings		158,995
9	Non-residential building		894,769
10	Roads		183,283
11	Sidewalks		136,035
12	Crosswalks		6059
13	Major thoroughfares		185,438
14	Highways		39,438
15	Railways		27,748
16	Paved parking lots		45,932
17	Unpaved parking lots		587
18	Cars		26,289
19	Trains		21,479
20	Stadium seats		27,296
Total			2,018,910

Table-2 : Class and sample description Kennedy Space Center (KSC) Hyperspectral Image

Salinas Hyperspectral Image: Salinas scene shown was collected by the 224-band AVIRIS sensor over Salinas Valley, California, and is characterized by high spatial resolution (3.7-m pixels). The area covered comprises 512 lines by 217 samples. After discarding the 20 water absorption bands (108–112, 154–167, 224), 204 bands are used for classification. There are 16 classes in the ground truth image.

Class	Description	GT Color	Number of Samples
1	Broccoli 1		2009
2	Broccoli 2		3726
3	Fallow 1		1976
4	Fallow 2		1394
5	Fallow 3		2678
6	Stubble		3959
7	Celery		3579
8	Grapes		11,271
9	Soil		6203
10	Corn		3278
11	Lettuce 1		1068
12	Lettuce 2		1927
13	Lettuce 3		916
14	Lettuce 4		1070
15	Vineyard 1		7268
16	Vineyard 2		1807
Total			54,129

Table-3 : Class and sample description Salinas Hyperspectral Image

The Indian Pines (IP) images: It has images with 145 × 145 spatial dimension and 224 spectral bands in the wavelength range of 400 to 2500 nm, out of which 24 spectral bands covering the region of water absorption have been discarded. The ground truth available is designated into 16 classes of vegetation.

Class	Description	GT Color	Number of Samples
1	Alfalfa		46
2	Corn-notill		1428
3	Corn-mintill		830
4	Corn		237
5	Grass-pasture		483
6	Grass-trees		730
7	Grass-pasture-mowed		28
8	Hay-windrowed		478
9	Oats		20
10	Soybean-notill		972
11	Soybean-mintill		2455
12	Soybean-clean		593
13	Wheat		205
14	Woods		1265
15	Buildings-Grass-Trees-Drives		386
16	Stone-Steel-Towers 2		93
Total			10,249

Table-4 : Class and sample description Indian Pines (IP) images

IV. PROPOSED METHOD

Multidimensional Convolution Neural Network (MCNN), Recurrent Convolution Neural Network (RCNN) and Multi-Dimensional Recurrent Neural Network (MDRNN) To verify the generalization abilities of both spectral and spectral-spatial CNNs, we investigate three convolution architectures that are gathered in Table 1. The spectral network (referred to as Multidimensional Convolution Neural Network (MCNN), this model performs the pixel-wise classification) is inspired by [33], whereas two spectral-spatial CNNs are denoted as Recurrent Convolution Neural Network (RCNN) and Multi-Dimensional Recurrent Neural Network (MDRNN) (these models perform the patch-wise classification of the central pixel in the corresponding patch, and the patch sizes

for Recurrent Convolution Neural Network (RCNN) for specific datasets were taken as suggested in). Although both Recurrent Convolution Neural Network (RCNN) and Multi-Dimensional Recurrent Neural Network (MDRNN) models benefit from the spectral and spatial information while classifying the central pixel in an input patch, Multi-Dimensional Recurrent Neural Network (MDRNN) can capture fine-grained spectral relations within the hyperspectral cube, as it exploits small (3 × 3 × 3) convolution kernels. It is in contrast to Recurrent Convolution Neural Network (RCNN) whose kernels span the entire spectrum, i.e., λ bands in the first convolution layer.

Multidimensional Convolution Neural Network Classifier

Input: TCRC: base classifier, T : the number of classifiers
 $X \in \mathbf{R}^{N \times M}$: Input training set and their label \mathbf{c} , λ , η : regularized parameter; \mathbf{y} : testing sample, $\Delta \mathbf{y}$: difference vector of \mathbf{y} , $\Delta \mathbf{X}$: difference vector of \mathbf{X}
 Weight initialization: $D_1(i) = 1/M, i = 1, 2, \dots, M$
For $t = 1$ to T
 Get new sample X^t under distribution D_t
 Construct new dictionary D^t by X^t
 Train TCRC using new sample D^t according to Eqs. (8-11)
 Calculate ε_t and b_t :
 $d_t = \|X + \Delta X \beta^t - D_c^t \alpha_c^t\|_2^2 - \min_{i \neq c} \|X + \Delta X \beta^t - D_i^t \alpha_i^t\|_2^2$
 $\varepsilon_t = \text{dot}(D_t, d_t)$ and $b_t = \max |d_t|$
 Calculate the residual error of \mathbf{y} :
 $r_m(\mathbf{y}) = \|\mathbf{y} + \Delta \mathbf{y} \beta^t - D_m^t \alpha_m^t\|_2^2, m = 1, 2, \dots, K$
 Choose ∂_t as: $\partial_t = \max\{(1/2b_t) \log((b_t - \varepsilon_t)/b_t + \varepsilon_t), 0\}$
 update the weight $D_{t+1}(i) = (D_t(i))/(Z_t) e^{\partial_t d_t}$ where Z_t is the normalization factor
End for: The weights $\{\partial_t\}_{t=1}^T$ after normalization
Classification: $\text{class}(\mathbf{y}) = \arg \min_{i=1,2,\dots,K} \sum_{t=1}^T \partial_t \|\mathbf{y} + \Delta \mathbf{y} \beta^t - D_i^t \alpha_i^t\|_2^2$

Model	Layer	Parameters	Activation
MCNN	Conv1	k: 200@(1 × 1 × 6) s: 1 × 1 × 1	ReLU
	Conv2	k: 200@(1 × 1 × 6) s: 1 × 1 × 3	ReLU
	Conv3	k: 200@(1 × 1 × 6) s: 1 × 1 × 2	ReLU
	Conv4	k: 200@(1 × 1 × 6) s: 1 × 1 × 2	ReLU
	FC1	# × 192	ReLU
	FC2 FC3	192 × 150 150 × c	ReLU Softmax
RCNN	Conv1 MP1	200@(w - 3 × w - 3 × λ) 2 × 2	ReLU
	Conv2	200@(2 × 2 × 200)	ReLU
	Conv3	c@(2 × 2 × 200)	Softmax
MDRNN	Conv1	24@(3 × 3 × 3)	ReLU
	Conv2	24@(3 × 3 × 3)	ReLU
	Conv3	24@(3 × 3 × 3)	ReLU
	FC1	# × 512	ReLU
	FC2	512 × 256	ReLU
	FC3 FC4	256 × 128 128 × c	ReLU Softmax

Table-5 : Configuration of Multidimensional Convolution Neural Network Classifier

V. CONCLUSION

Deep learning approaches have turned into a laid out apparatus in both hyperspectral image information order and unmixing, yet the absence of ground-truth information is a significant hindrance, which hampers the reception of such huge limit students and makes their speculation capacities problematic in commonsense applications. We presented the profound gatherings for HSI examination that not just advantage from various profound design progresses catching unearthly and ghastly spatial qualities inside the info HSI yet additionally from administered students going about as effective fusers of base models.. The hyperspectral images contain wide band of information available as the spatial and spectral information. These features serve better for implementation of the accurate and real time image classification and object detection applications. These are certain challenges that are addressed including the high dimensional data and the limitation of the training data for making the system learn the image classification and performing object detection. The Ensemble deep learning approach for the image classification of hyperspectral images is proposed with the view to improve the accuracy of image classification over homogeneous and heterogeneous

data sets of hyperspectral Images. The proposed ensemble learning method is applied for improving the class boundary and the help in real time object recognition and detection in hyperspectral images.

VI. REFERENCES

- [1]. J. M. Bioucas-Dias, A. Plaza, G. Camps-Valls, P. Scheunders, N. Nasrabadi, and J. Chanussot, "Hyperspectral remote sensing data analysis and future challenges," *IEEE Geoscience and Remote Sensing Magazine*, vol. 1, no. 2, pp. 6–36, 2013.
- [2]. W. Hu, Y. Huang, L. Wei, F. Zhang, and H. Li, "Deep convolutional neural networks for hyperspectral image classification," *Journal of Sensors*, 2015.
- [3]. Y. S. Chen, J. L. Jiang, C. Y. Li, X. P. Jia, and P. Ghamisi, "Deep feature extraction and classification of hyperspectral images based on convolutional neural networks," *IEEE Transactions on Geoscience and Remote Sensing*, vol. 54, no. 10, pp. 6232–6251, 2016.
- [4]. G. E. Hinton, S. Osindero, and Y. Teh, "A fast learning algorithm for deep belief nets," *Neural Computation*, vol. 18, pp. 1527–1554, 2006.
- [5]. S. Lee, S. P. S. Prakash, M. Cogswell, V. Ranjan, D. Crandall, and D. Batra, "Stochastic multiple choice learning for training diverse deep ensembles," in *Advances in Neural Information Processing Systems*, 2016, pp. 2119–2127.
- [6]. P. Yadollahpour, D. Batra, and G. Shakhnarovich, "Discriminative re-ranking of diverse segmentations," in *Proceedings of IEEE Conference on Computer Vision and Pattern Recognition*, 2013, pp. 1923–1930.
- [7]. Guzman-Rivera, D. Batra, and P. Kohli, "Multiple choice learning: Learning to produce multiple structured outputs," in *Advances in Neural Information Processing Systems*, 2012, pp. 1799–1807.
- [8]. K. Gimpel, D. Batra, C. Dyer, and G. Shakhnarovich, "A systematic exploration of diversity in machine translation," in *Proceedings of the 2013 Conference on Empirical Methods in Natural Language Processing*, 2013, pp. 1100–1111.
- [9]. Filippi, A. M., Archibald, R., Bhaduri, B. L., & Bright, E. A. (2009). Hyperspectral agricultural mapping using support vector machine- based endmember extraction (SVM-BEE). *Optics Express*, 17(26), 23823–23842.
- [10]. Jones, T. G., Coops, N. C., & Sharma, T. (2010). Assessing the utility of airborne hyperspectral and LiDAR data for species distribution mapping in the coastal Pacific Northwest, Canada. *Remote Sensing of Environment*, 114(12), 2841–2852.
- [11]. Lavanya, A., & Sanjeevi, S. (2012). An improved band selection technique for hyperspectral data using factor analysis. *Journal of the Indian Society of Remote Sensing*, 41(2), 199–211.
- [12]. Harsanyi, J. C., & Chang, C. I. (1994). Hyperspectral image classification and dimensionality reduction: an orthogonal subspace projection approach. *IEEE Transactions on Geoscience and Remote Sensing*, 32(4), 779–785.
- [13]. Chirici, G., Giuliarelli, D., Biscontini, D., Tonti, D., Mattioli, W., Marchetti, M., et al. (2011). Large-scale monitoring of coppice forest clearcuts by multitemporal very high resolution satellite imagery. A case study from central Italy. *Remote Sensing of Environment*, 115, 1025–1033.
- [14]. Henriques, A. P. M., Do 'ria, N. A. D., & Amaral, R. F. (2010). Classification of multispectral images in coral environments using a hybrid of classifier ensembles. *Neurocomputing*, 73(7–9), 1256–1264.
- [15]. Huang, X., Lu, Q., & Zhang, L. (2014). A multi-index learning approach for classification of high-resolution remotely sensed images over urban areas. *ISPRS Journal of Photogrammetry and Remote Sensing*, 90, 36–48.

- [16]. Myint, S. W., Gober, P., Brazel, A., Grossman-Clarke, S., & Weng, Q. (2011). Per-pixel vs. object-based classification of urban land cover extraction using high spatial resolution imagery. *Remote Sensing of Environment*, 115(5), 1145–1161.
- [17]. Pu, R., & Landry, S. (2012). A comparative analysis of high spatial resolution IKONOS and WorldView-2 imagery for mapping urban tree species. *Remote Sensing of Environment*, 124, 516–533.
- [18]. Erener, A. (2013). Classification method, spectral diversity, band combination and accuracy assessment evaluation for urban feature detection. *International Journal of Applied Earth Observation and Geoinformation*, 21, 397–408. <https://doi.org/10.1016/j.jag.2011.12.008>.
- [19]. Wei, Y., Xiao, G., Deng, H., & Chen, H. (2015). Hyperspectral image classification using FPCA-based kernel extreme learning machine. *Optik*, 126, 3942–3948.
- [20]. Chakraborty, A., Sachdeva, K., & Joshi, P. K. (2016). Mapping longterm land use and land cover change in the central Himalayan region using a tree-based ensemble classification approach. *Applied Geography*, 74, 136–150.
- [21]. Ghoggali, N., & Melgani, F. (2008). Genetic SVM Approach to Semisupervised Multitemporal Classification. *IEEE Geoscience and Remote Sensing Letters*, 5(2), 212–216.
- [22]. Gu, B., & Sheng, V.S. (2016). A robust regularization path algorithm for v-support vector classification. *IEEE Transactions on Neural Networks and Learning Systems*.
- [23]. Volpi, M., Tuia, D., Bovolo, F., Kanevski, M., & Bruzzone, L. (2013). Supervised change detection in VHR images using contextual information and support vector machines. *International Journal of Applied Earth Observation and Geoinformation*, 20, 77–85.

Cite this article as :

Parul Bhanarkar, Dr. Salim Y. Amdani, "Deep Learning Ensemble Model for Hyperspectral Image Classification", *International Journal of Scientific Research in Science, Engineering and Technology (IJSRSET)*, Online ISSN : 2394-4099, Print ISSN : 2395-1990, Volume 9 Issue 2, pp. 12-18, March-April 2022. Journal URL : <https://ijsrset.com/IJSRSET22923>